

# Modal Analysis of Anisotropic Diffused-Channel Waveguide by a Scalar Finite Element Method

Marcos A. R. Franco, Angelo Passaro, Francisco Sircilli Neto

Centro Técnico Aeroespacial - CTA/IEAv, Rod. Tamoios, km.5,5 - CEP. 12228-840, São José dos Campos, SP, Brazil,

José R. Cardoso

Laboratório de Eletromagnetismo Aplicado - LMAG - PEA - EPUSP  
Av. Prof. Luciano Gualberto, Trav.3, no.158 - CEP05508-900 - São Paulo, SP, BRAZIL

José M. Machado

Depto. de Ciências da Computação e Estatística IBILCE - UNESP - CP 136 - CEP.: 15054-000 - S. J. Rio Preto - SP - Brazil

**Abstract** – A procedure to model optical diffused-channel waveguides is presented in this work. The dielectric waveguides present anisotropic refractive indexes which are calculated from the proton concentration. The proton concentration inside the channel is calculated by the anisotropic 2D-linear diffusion equation and converted to the refractive indexes using mathematical relations obtained from experimental data. The arbitrary refractive index profile is modeled by a nodal expansion in the base functions. The TE and TM-like propagation properties (effective index) and the electromagnetic fields for well-annealed proton-exchanged (APE) LiNbO<sub>3</sub> waveguides are computed by the finite element method.

**Index terms** – Finite element methods, nonhomogeneous loaded waveguides, optical strip waveguides, anisotropic media, diffusion processes.

## I. INTRODUCTION

Many optical devices of technological importance use diffused channel waveguides which present arbitrary refractive index profiles. Annealed proton-exchanged (APE) LiNbO<sub>3</sub> optical waveguides are currently used in many integrated optic devices: fiberoptic gyroscopes (FOG), electrooptic, acoustooptic and magneto-optic modulators, sensors and switches, second harmonic generators, cable television (CATV), signal distributions and long haul telecommunications.

The computation of the waveguide modes dispersion and the modeling of the APE process of diffused channel waveguides are the central problems for the design of such devices.

The APE guides have the desirable property of single polarization because the APE process changes only the refractive index for the extraordinary polarization. This process results in a continuous variation of the extraordinary refractive index.

Scalar and vector finite element methods (FEM) for modal analysis in homogeneous waveguides with isotropic or anisotropic refractive indexes have been described by several authors [1]-[5]. References [6]-[12] present the application of numerical formulations for isotropic and anisotropic diffused waveguides.

Notwithstanding the great number of papers on the calculation of the electromagnetic properties of anisotropic-diffused optical

waveguides and on models proposed to simulate the manufacturing process of APE waveguides, there is a lack of published works on coupled calculations.

This work presents the procedure we are adopting to study the electromagnetic propagation modes in anisotropic diffused-channel waveguides. Our approach covers the complete process from the production to the electromagnetic characterization of well-annealed proton exchanged waveguide devices.

The scalar FEM formulation to compute the propagation modes with a continuously varying refractive index inside a finite element and the procedure to define the refractive index are presented in the next two sections. The results are presented in Section IV.

## II. FINITE ELEMENT MODEL

A full-wave analysis of shielded waveguide structures, with electric anisotropic materials can be described by the following vector equations:

$$\nabla \times \nabla \times \vec{E} - k_0^2 \vec{E}_r \vec{E} = 0 \quad (1)$$

$$\nabla \times (\vec{E}_r \nabla \times \vec{H}) - k_0^2 \vec{H} = 0 \quad (2)$$

where  $k_0$  is the free space wavenumber, the relative permeability of the waveguide material is assumed equal 1, and  $\vec{E}_r$  is the relative permittivity:

$$\vec{E}_r = \begin{bmatrix} n_x^2(x, y) & 0 & 0 \\ 0 & n_y^2 & 0 \\ 0 & 0 & n_z^2 \end{bmatrix} \quad (3)$$

$n_x, n_y, n_z$  are the refractive indexes in the x, y, and z directions, respectively.

We consider lossless diffused-channel waveguides where the light propagates along the z direction with a harmonic dependence of the position given by:

$$\vec{V} = \vec{V}_0(x, y) e^{-j k_z z},$$

where  $\vec{V}$  represents either the electric or magnetic fields and  $k_z$  is the propagation constant.

The  $E^x$  and the  $E^y$  modes are generally used in integrated optics. The  $E^x$  mode is well approximated by the TE mode (for which  $E_y = 0$  and  $E_x$  is the leading function) and the  $E^y$  mode by the TM mode ( $H_y = 0$ ,  $H_x$  is the leading function).

Manuscript received November 03, 1997

M.A.R. Franco, fax +55 12 344-1177, marcos@ieav.cta.br; A. Passaro, angelo@ieav.cta.br; F. S. Neto, sircilli@ieav.cta.br; J. R. Cardoso, cardoso@pea.usp.br; J. M. Machado, marcio@nimitz.dece.ibilce.unesp.br.

This work was supported in part by the FAPESP - Fundação de Amparo à Pesquisa do Estado de São Paulo, process No. 95/06608-0

In the TE and TM approximations, the following generalized two-dimensional wave equation is obtained from (1) and (2):

$$\frac{\partial^2(A\phi)}{\partial x^2} + B \frac{\partial^2\phi}{\partial y^2} + (k_0^2 D - \beta_z^2 C) \phi = 0 \quad (4)$$

where the state variable assumes  $\phi = E_x$  for the  $E^x$  mode and  $\phi = H_x$  for the  $E^y$  mode. The parameters A, B, C, and D for the  $E^x$  and  $E^y$  modes are presented in Table I.

TABLE I

PARAMETERS FOR THE  $E^x$  AND  $E^y$  MODES PRESENTED IN (4). ( $n_x, n_y, n_z$ ) ARE THE REFRACTIVE INDEXES ALONG THE CARTESIAN AXES.

mode	A	B	C	D
$E^x$	$D/n_z^2$	1	1	$n_x^2(x, y)$
$E^y$	$D/n_y^2$	$1/n_z^2$	$1/n_y^2$	1

The application of the Weighted Residual Method with the Galerkin approximation in (4) yields the matrix equation:

$$[K]\{\phi\} = n_{eff}^2 [M]\{\phi\} \quad (5)$$

where  $n_{eff} = k_z/k_0$  is the effective index.

The extraordinary refractive index  $n_x$  varies with the (x,y) coordinates inside the diffused channel and remains constant elsewhere. Both the state variable  $\phi$  and the refractive index  $n_x$  inside the diffused channel were modeled using the nodal approximation:

$$\phi = \sum_{k=1}^{Np} N_k \phi_k = \{N\}\{\phi\}^T,$$

$$n_x^2 = \sum_{k=1}^{Np} N_k n_{xk}^2 = \{N\}\{n_x^2\}^T,$$

where  $Np$  is the number of nodal points of the element,  $\{N\}$  represents a complete set of base functions for the finite element used,  $\{\}$  represents a row matrix and  $\{\}^T$  stands for a transposed matrix. Therefore, the matrices  $[K]$  and  $[M]$  for triangular finite elements are:

$$[K] = 2\Delta k_0^2 \iint_{\zeta_1 \zeta_2} D \{N\}^T \{N\} d\zeta_1 d\zeta_2$$

$$- \sum_{i,j=1}^3 \left( \frac{b_i b_j}{2\Delta} \iint_{\zeta_1 \zeta_2} A \frac{\partial \{N\}^T}{\partial \zeta_i} \frac{\partial \{N\}}{\partial \zeta_j} d\zeta_1 d\zeta_2 \right)$$

$$- \delta \sum_{i,j=1}^3 \left( \frac{b_i b_j}{2\Delta} \iint_{\zeta_1 \zeta_2} \frac{\partial \{N\}^T}{\partial \zeta_i} \frac{\partial A}{\partial \zeta_j} \{N\} d\zeta_1 d\zeta_2 \right)$$

$$- \sum_{i,j=1}^3 \left( \frac{c_i c_j}{2\Delta} B \iint_{\zeta_1 \zeta_2} \frac{\partial \{N\}^T}{\partial \zeta_i} \frac{\partial \{N\}}{\partial \zeta_j} d\zeta_1 d\zeta_2 \right)$$

$$[M] = 2\Delta k_0^2 C \iint_{\zeta_1 \zeta_2} \{N\}^T \{N\} d\zeta_1 d\zeta_2,$$

where  $\Delta$  is the triangle area,  $\zeta_i$  are the independent homogeneous coordinates and  $b_i$  and  $c_i$  are the homogeneous system coordinate-transformation coefficients. The parameter  $\delta$  assumes either the value 1 for diffused channels, or zero for homogeneous materials. For the latter, the matrix  $[K]$  reproduces the usual scalar Helmholtz equation matrices.

In the homogeneous coordinate system the integrals over the unitary triangle do not depend of the triangle geometry; such integrals were previously evaluated as in [20].

The method of calculation of the refractive index  $n_x$  in the nodal points is presented in the next section.

### III. REFRACTIVE INDEX MODEL

The proton exchange (PE) process in  $\text{LiNbO}_3$  is carried out by placing the  $\text{LiNbO}_3$  uniaxial crystal in a proton-rich bath, e.g. benzoic acid, kept at fixed temperature. Typically,  $150^\circ\text{C} < T < 250^\circ\text{C}$  and exchange times of  $5 \text{ min} < t < 5 \text{ hours}$ . The hydrogen ions of the bath and the lithium ions of the crystal migrate, therefore, increasing the proton concentration in the crystal and reducing the lithium concentration.

The PE process in pure benzoic acid yields an increase of 0.12 in the value of the  $\text{LiNbO}_3$  extraordinary refractive index for  $\lambda = 0.6328 \mu\text{m}$  while the ordinary index remains almost unchanged [13], [16], [17]. Moreover, there is a reduction of the electrooptic coefficient and the propagation losses increase [14].

The normalized proton concentration after the PE process is approximated in this work by a step function. The effective exchanged layer depth follows the diffusion law:

$$d = 2\sqrt{D_{PE} t},$$

where  $D_{PE}$  is the PE diffusion coefficient and  $t$  is the PE diffusion time. The channel width is supposed to be equal to the mask opening used in the PE process. Such approximations are supported by experimental results [13]-[18].

The protons are redistributed inside the substrate by an annealing process carried out in normal atmosphere at temperatures above  $300^\circ\text{C}$ . The annealing process restores the electrooptic coefficient and reduces both the optical damage and propagation losses.

Well-chosen parameters for the annealing process are essential to manufacture high-quality diffused waveguides.

Complex changes in the  $\text{LiNbO}_3$  crystalline structure occur during the annealing process. At the end of the PE process the PE channel presents the  $\beta$ -phase crystalline structure due to the high proton concentration. The annealing process promotes a redistribution of the proton and Li ions inside the substrate. Therefore, there is a decrease in the protons concentration in the PE channel and an increase in the proton concentration in its vicinity. The crystalline structure changes as the proton concentration varies [14]-[16], [18]. We focus our attention to the  $\alpha$ -phase crystal waveguides for which there is less than twenty percent lithium ions exchanged by protons (well-annealed crystals).

The simulation of the annealing process for well-annealed waveguides is supposed to follow the 2D-anisotropic diffusion equation with a finite source (PE layer):

$$\frac{\partial C^H}{\partial t} = \frac{\partial}{\partial x} \left( D_{ax} \frac{\partial C^H}{\partial x} \right) + \frac{\partial}{\partial y} \left( D_{ay} \frac{\partial C^H}{\partial y} \right) \quad (6)$$

We assumed  $C^H = 0.8$  in the PE rectangular channel at the beginning of the annealing process (initial condition).

The dependence of the annealing diffusion coefficients on the proton and Li ion concentrations has been studied by several authors [15], [21]-[22]. However, there is a lack of data for the diffusion coefficients in the literature. Additionally, experimental concentration profiles for well-annealed waveguides are well fitted by using (6) [14], [16], [23], [24]. Therefore, although the annealing diffusion coefficients,  $D_{ax}$  and  $D_{ay}$ , depend on the proton and Li ions concentrations they were assumed to be constant in our calculations.

Equation (6) is solved by the FEM. The  $C^H$  concentrations obtained are used to calculate the extraordinary refractive index in the finite element mesh points inside the  $\text{LiNbO}_3$ .

Several authors propose mathematical relations between the extraordinary refractive index and the proton concentration [14]-[16]:

$$n_x(C) = n_{sx} + \Delta n_x(C),$$

where  $n_{sx}$  is the bulk extraordinary refractive index of the  $\text{LiNbO}_3$  (substrate),  $C$  is a normalized concentration of protons, and  $\Delta n_x(C)$  is the refractive index change due to the concentration  $C$ .

Reference [15] suggests the following model:

$$\Delta n_x(C) = \Delta n_x^{PE} [1 - e^{-\sigma C}], \quad (7)$$

where  $\Delta n_x^{PE}$  is the maximum refractive index change induced by the PE process,  $0 \leq C \leq 1$  and  $\sigma = 11$ . We redefined the limits for the concentration in this work as:

$$0 < C < C_{max}^H$$

where  $C_{max}^H = 0.16$  corresponds to the maximum normalized concentration for well-annealed waveguides. We obtained a  $\sigma$  value of 1.3 from the fit of (7) to the available experimental data for well-annealed waveguides [14]; it was used in our computations.

Reference [16] suggests a linear relation to represent the refractive index for well-annealed waveguides:

$$\Delta n_x(C) = 0.05 C. \quad (8)$$

The effective indexes of the waveguides were computed using either (7) or (8). The results are shown in Section IV.

The following expression for the dispersion of the refractive index in well-annealed waveguides is assumed for the study of propagation modes with arbitrary wavelength [16]:

$$n_x(\lambda) = n_{sx} + \Delta n_x(C) \left( 0.78912 + \frac{0.06293}{(\lambda^2 - 0.07852)} + 0.048 \lambda^2 \right)$$

#### IV. RESULTS

The program implementation was validated by comparing our results with those of Koshiba for a rib channel filled with an anisotropic material [1].

The results presented in this section were obtained using approximately 3500 node points (first-order triangular Lagrange-type elements). The same FE mesh was utilized to solve both the diffusion and the electromagnetic equations in order to take advantage of the previously calculated proton concentration at the nodal points.

We assumed for the PE process a chemical attack in pure benzoic acid with the following diffusion coefficients for the x and z-cut crystals, respectively:  $D_{PEx}(190^\circ\text{C}) = 0.09188 \mu\text{m}^2/\text{h}$  [17] and  $D_{PEz}(180^\circ\text{C}) = 0.027 \mu\text{m}^2/\text{h}$  [25]. In both cases, the mask opening was of  $6 \mu\text{m}$ . The PE channel effective depth was of  $0.3 \mu\text{m}$  for both the x and z-cuts.

The diffusion coefficients adopted for the annealing process were  $D_a(\text{x-cut}) = 0.92 \mu\text{m}^2/\text{h}$  and  $D_a(\text{z-cut}) = 0.77 \mu\text{m}^2/\text{h}$  [14]. The annealing time is four hours at  $360^\circ\text{C}$ .

Figs. 1 and 2 show the effective index variation as a function of the annealing time for both x and z-cut  $\text{LiNbO}_3$ .

Figs. 3 and 4 show the waveguides dispersion curves and the cutoff limits.

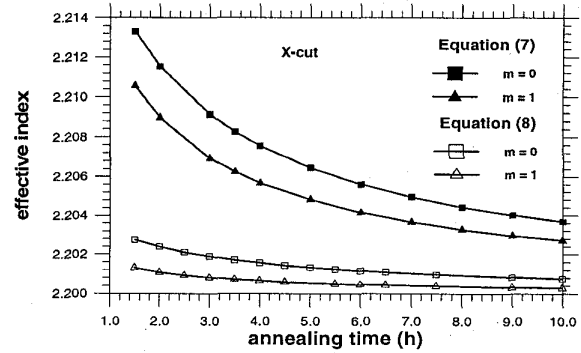


Fig. 1: Behavior of the effective index as a function of the annealing time for the x-cut  $\text{LiNbO}_3$  (wavelength =  $0.6328 \mu\text{m}$ )

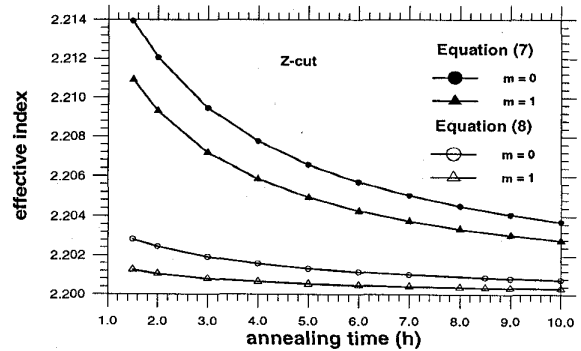


Fig. 2: Behavior of the effective index as a function of the annealing time for the z-cut  $\text{LiNbO}_3$  (wavelength =  $0.6328 \mu\text{m}$ )

The results obtained using either (7) or (8) to calculate the refractive index from the proton concentration are quite different, as shown in Figs. 1-4. Moreover, several propagation modes were obtained using (7), but no more than three modes

were guided in the diffused channel when the computation was carried out using (8).

Since the same PE channel effective depth was used, only slight differences were obtained for the x and z-cut results.

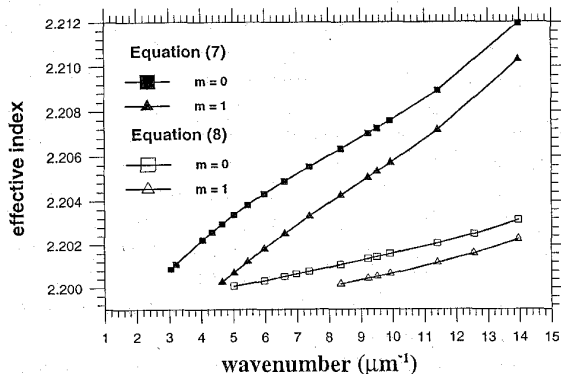


Fig. 3 Dispersion curves (x-cut) obtained from (7) and (8).

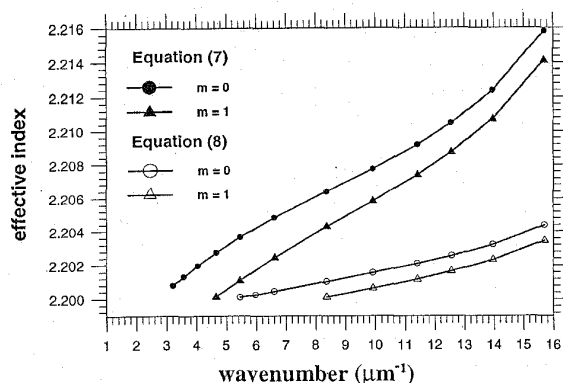


Fig. 4 Dispersion curves (z-cut) obtained from (7) and (8).

## V. CONCLUSIONS

The procedure presented in this paper was used to study well-annealed proton exchanged waveguides for which only the extraordinary index profile is arbitrary. The FE equations presented can be easily extended to study the electromagnetic propagation in materials with an arbitrary index profile in the y and z directions.

The two proton concentration to refractive index coupling methods yield quite different results for the effective index. Therefore, efforts should be undertaken to obtain a better definition for the relationship between the proton concentration in the LiNbO<sub>3</sub> and the extraordinary refractive index.

## REFERENCES

- [1] M. Koshiba, K. Hayata, M. Suzuki, "Approximate scalar finite-element analysis of anisotropic optical waveguides," *Electron. Lett.*, vol. 18, pp. 411-413, May, 1982.
- [2] M. Koshiba, H. Saitoh, M. Eguchi, K. Hirayama, "Simple scalar finite element approach to optical rib waveguides," *IEE Proc. - J*, vol. 139, n. 2, pp. 166-171, 1992.
- [3] M. Koshiba, "Computer-aided design of integrated optical waveguide devices", in *Finite Element Software for Microwave Engineering*, T. Itoh, G. Pelosi and P.P. Silvester, Eds. Wiley Series in Microwave and Optical Engineering, John Wiley & Sons, New York, 1996, pp. 79-81.
- [4] A.C. Polycarpov, M.R. Lyons and C.A. Balanis, "Finite element analysis of MMIC waveguide structures with anisotropic substrates," *IEEE Trans. Microwave Theory Tech.*, vol. 44, n. 10, pp. 1650-1662, 1996.
- [5] B.M.A. Rahman, F.A. Fernandez and J. Brian Davies, "Review of finite element methods for microwave and optical waveguides," *Proc. IEEE*, vol. 79, n. 10, pp. 1442-1448, 1991.
- [6] J.P. Donnelly and S.D. Lau, "Generalized effective index series solution analysis of waveguide structures with positionally varying refractive index profiles," *IEEE J. Quantum Electron.*, vol. 32, n.6, pp. 1070-1079, 1996.
- [7] N. Schulz, K. Bierwirth, F. Arndt and U. Köster, "Rigorous finite-difference analysis of coupled channel waveguides with arbitrary varying index profile," *J. Lightwave Technol.*, vol. 9, n.10, pp. 1244-1253, 1991.
- [8] N. Zhu, R. Wang and Z. Wang, "Variational analysis of eigenmodes of integrated optical waveguides and applications," *Science in China (Series A)*, vol. 38, N. 5, pp. 608-617, 1995.
- [9] R.B. Wu and C.H. Chen, "A scalar variational conformal mapping technique for weakly guiding dielectric waveguides," *IEEE J. Quantum Electron.*, vol. QE-22, n. 5, pp. 603-609, 1986.
- [10] Ch. Pichot, "Exact numerical solution for the diffused channel waveguide," *Opt. Commun.*, vol. 41, n. 3, pp. 169-173, 1982.
- [11] F.A. Katsiriku, B.M.A. Rahman and K.T.V. Grattan, "Finite element analysis of diffused anisotropic optical waveguides," *J. Lightwave Technol.*, vol. 14, n. 5, pp. 780-786, 1996.
- [12] C.L.S. Souza Sobrinho and A.J. Giarola, "Analysis of a dielectric channel waveguide diffused in an anisotropic substrate with a Gaussian-Gaussian index of refraction profile using the finite difference method," *Proceedings of the 1993 SBMO International Microwave Conference*, Brazil, Aug., 1993.
- [13] J.L. Jackel, C.E. Rice and J.J. Veselka, "Proton exchange for high-index waveguides in LiNbO<sub>3</sub>," *Appl. Phys. Lett.*, vol. 41, n.7, pp. 607-608, 1982.
- [14] M.M. Howerton, W.K. Burns, P.R. Skeath and A.S. Greenblatt, "Dependence of Refraction Index on Hydrogen Concentration in Proton Exchanged LiNbO<sub>3</sub>," *IEEE J. Quantum Electron.*, vol. 27, n. 3, pp. 593-601, 1991.
- [15] S.T. Vohra, A.R. Michelson and S.E. Asher, "Diffusion characteristics and waveguiding properties of proton-exchanged and annealed LiNbO<sub>3</sub> channel waveguides," *J. Appl. Phys.*, vol. 66, n.11, pp. 5161-5173, 1989.
- [16] X. F. Cao, R.V. Ramaswamy and R. Srivastava, "Characterization of Annealed Proton Exchanged LiNbO<sub>3</sub> Waveguides for Nonlinear Frequency Conversion," *J. Lightwave Technol.*, vol. 10, pp. 1302-1313, 1992.
- [17] K. M. Kissa, P.G. Suchoski and D.K. Lewis, "Accelerated Aging of Annealed Proton-Exchanged Waveguides," *J. Lightwave Technol.*, vol. 13, pp. 1521-1529, July 1995.
- [18] J.M. Cabrera, J. Olivares, M. Carrascosa, J. Rams, R. Müller and E. Dieguez, "Hydrogen in lithium niobate," *Advances in Physics*, vol. 45, n. 5, pp. 349-392, 1996.
- [19] M. Koshiba and X.P. Zhuang, "An efficient finite-element analysis of magnetooptic channel waveguides," *J. Lightwave Technol.*, vol. 11, n. 9, pp. 1453-1458, 1993.
- [20] M.A.R. Franco, A. Passaro and J.M. Machado, "MATHEMATICA notebook for computing tetrahedral finite element shape functions and matrices for the Helmholtz equation," *IEEE Trans. Magn.*, Sept 1998, in press.
- [21] J. Nikolopoulos and G.L. Yip, "Accurate Modeling of the Index profile in annealed proton-exchanged LiNbO<sub>3</sub> waveguides," *SPIE*, vol. 1583, Integrated Optical Circuits, pp. 71-82, 1991.
- [22] M.L. Bortz and M.M. Fejer, "Annealed proton-exchanged LiNbO<sub>3</sub> waveguides," *Opt. Lett.*, vol. 16, n. 23, pp. 1844-1846, 1991.
- [23] G.R. Paz-Pujalt, D.D. Tuschel, G. Braunstein, T. Blanton, S.T. Lee and L.M. Salter, "Characterization of proton exchange lithium niobate waveguides," *J. Appl. Phys.*, vol. 76, n. 7, pp. 3981-3987, 1994.
- [24] H. Ahlfeldt, "Nonlinear optical properties of proton-exchanged waveguides in z-cut LiTaO<sub>3</sub>," *J. Appl. Phys.*, vol. 76, n. 6, pp. 3255-3260, 1994.
- [25] D.F. Clark, A.C.G. Nutt, K.K. Wong, P.J.R. Laybourn and R.M. De LaRue, "Characterization of proton-exchange slab optical waveguides in z-cut LiNbO<sub>3</sub>," *J. Appl. Phys.*, vol. 54, n. 11, pp. 6218-6220, 1983.